

Août 1973

LRP 65/73

LASER SCATTERING MEASUREMENTS ON A
ROTATING MAGNETIC FIELD PINCH

Z.A. Pietrzyk, A. Heym, F. Hofmann, A. Lietti
P. Boulanger and D.W. Ignat

Centre de Recherches en Physique des Plasmas
ECOLE POLYTECHNIQUE FEDERALE DE LAUSANNE

LASER SCATTERING MEASUREMENTS ON A
ROTATING MAGNETIC FIELD PINCH

Z.A. Pietrzyk, A. Heym, F. Hofmann, A. Lietti
P. Boulanger and D.W. Ignat

Abstract

Previous investigations of a plasma subjected to a rotating magnetic field are extended to include data from laser light scattering. The electron temperature and density are measured in the center of the discharge as a function of time. The measurements are compared with a MHD model of the experiment.

Introduction

Pinch experiments involve the sudden application of a magnetic field to an ionized gas. In linear experiments the applied field commonly follows a single direction: axial for the θ -pinch and azimuthal for the z-pinch. The screw pinch combines the two so the field takes a helical shape.

It is also possible that the pinching field does not follow a single direction but instead rotates on the plasma surface. Such a configuration can be thought of as combined rf z-and θ -pinches with the two dephased by 90° . The rotating magnetic field pinch configuration has received some theoretical and experimental investigation (WEIBEL, 1960; TROYON, 1971; JONES et al., 1968; BERNEY et al., 1971; IGNAT et al., 1973; HOFMANN, 1971a).

Previous experimental work has included electrical, spectroscopic, optical, magnetic probe, and interferometric diagnostics of the interaction between the plasma and the applied magnetic field. We report here the results obtained from the scattering of ruby laser light at 90° . The method has allowed determination of the electron temperature and density in the center of the tube as a function of time.

Apparatus

The discharge tube has a 15 cm diameter. The distance between the electrodes for drawing z-currents is about 85 cm. The rf magnetic field oscillates near 2.5 MHz and grows to a maximum amplitude of approximately 2 kG in 5 μ sec. One third maximum amplitude is reached in about 1 μ sec. Two unidirectional z-current pulses of 22 kA peak current and lasting 5 μ sec with a 5 μ sec separation preionize the plasma. For more details, see IGNAT et al. (1973).

The scattering measurement, which is diagramed in Fig. 1, employs a Q-switched ruby laser capable of delivering 2 Joules in a pulse of 25 nsec FWHM. A 100 cm focal length lens focuses the output beam on a cleaning diaphragm. Thereafter another 100 cm focal length lens images the dia-

phragm in the axial middle of the discharge tube by directing the laser beam along the tube axis.

The scattered signal is observed at 90° to the incident beam. A 7 \AA bandwidth interference filter placed in front of the photomultiplier achieves wavelength selection. A very small portion of the laser beam passes straight through the final prism. This light provides two weak beams for monitoring the time of laser firing and the shape of the pulse. The first beam, after detection by a photodiode, appears on the same oscilloscope trace as the external probe sensing θ -current. This allows accurate determination of the laser firing time with respect to the progress of the applied pinching field. The second beam, delayed for 140 nsec by a light guide, enters the photomultiplier directly without passing through the wavelength selection filter. This allows calibration of the photomultiplier and amplifier with a signal having the same shape and similar amplitude as the scattered signal. It also gives the laser power in each pulse. Measurements were done with the same discharge conditions as examined previously (IGNAT et al., 1973), that is, 20 mTorr D_2 filling pressure and a 28 kV charging of the capacitors in the rf line.

Most experiments are in the Thomson scattering regime ($\alpha = (k\lambda_D)^{-1} \leq 0.5$). In these cases we fit the measured spectra to a Gaussian curve with a least-squares program to obtain the plasma parameters. For the few cases in the collective scattering regime ($\alpha \approx 1$) we analyze the data with Kegel's curves (KEGEL, 1965). In these instances the curve shape gives an independent check on the electron density so that the total scattering cross section for both the Thomson scattering and the collective scattering conditions could be determined (KUNZE, 1968).

The total scattering cross section as calibrated from the shape of the spectra is about 30 o/o higher than a calibration based on Rayleigh scattering from N_2 . The errors involved in each method if added span 30 o/o.

Measurements

In Figs 2 and 3 the round circles denote the electron density and temperature at plasma center as inferred from laser scattering on the 20 mTorr D_2

experiment. The interferometric measurements of Heym (HEYM, 1968; IGNAT et al., 1973), which represent electron area densities converted to volume density by assuming axial uniformity of the plasma, appear as a dashed line in Fig. 2. The two techniques agree well except near the time of maximum electron density. We believe the discrepancy between the scattering and interferometry data can be attributed to lack of axial uniformity in the plasma due to the influence of the ends on both the pinching field and the plasma parameters. These effects would make the time of the implosion different along the axis and lead to a smearing in time of the density peak derived from the interferometer.

This problem may have been compounded by slow variations in the characteristics of the rf line generator over the year separating the two types of measurement. Finally, any canting of the interferometer beam with respect to the discharge axis would also contribute to discrepancy at the time of maximum implosion.

The measured temperature behaves consistently with the density in that the maximum comes about the same time. The temperature is low, but with the high densities obtained, the plasma pressure is comparable with the rf magnetic pressure. We define β to be the plasma kinetic pressure at $r = 0$ divided by the magnetic pressure at the wall

$$\beta = n k(T_e + T_i) / ((B_\theta^2 + B_z^2) / 2 \mu_0).$$

In the above formula, n is electron density, k is Boltzmann's constant, $T_{e,i}$ is the electron (ion) temperature, $B_{\theta,z}$ represent the rf field at the wall, and μ_0 is the permittivity of free space. We assume that the electron and ion temperatures are equal since this has been true at small radius in our MHD simulations of the experiment. Then at peak compression β reaches 3.6 and falls to 0.52 at 4 μs and .08 at 5 μs . We should remark that since the pinch is not in equilibrium these numbers do not have the standard interpretation. We quote them to give an idea of the plasma pressure scaled to the pinch field.

Measurements and computations (BERNEY et al., 1971; HOFMANN, 1971a,b; IGNAT et al., 1973) regarding the rotating magnetic field pinch have established (1) the presence of large anomalous resistivity, (2) the fact that most of the plasma current flows very near the wall. Measurements of the total number of electrons in discharges made at low (< 60 mTorr) filling pressure have shown that sometime during the experiment there is a large flux of particles from the wall. For example, with a 20 mTorr filling of D_2 , the number of electrons in the tube measured by the interferometer 5 μ sec into the main discharge is 50 o/o more than the number corresponding to the filling density. There is no experimental information on the history of the flux. All extra particles could enter during the preionization phase, or most could enter later with any sort of time dependence.

Using the measurements now available, we have attempted to clarify this final point with the aid of the three fluid, one dimensional MHD simulation code (HOFMANN, 1971a,b). We assume that from the discharge tube wall there is a steady flow of D atoms into the vacuum region, and that this gas immediately becomes fully ionized. We plot in Figs 2 and 3 the predictions of the MHD code assuming fluxes (FLX) of 0., 0.6 and 1.0×10^{15} electron-ion pairs / $cm^2 \mu$ sec at the discharge tube wall as well as the results of assuming that all extra atoms entered before the discharge. The computation includes anomalous resistivity as was done previously ($\alpha = 0.3$ in the notation of IGNAT et al., 1973, or $\alpha_{BUN} = 0.3$ in the notation of HOFMANN, 1971a) and also axial heat conduction.

Similarly in Fig. 4 we give the situation for the radial density profile at $t = 5 \mu$ s. It follows from these comparisons that the extra particles come in during the discharge and not before. Most probably the flux is time dependent in a manner we have not tried to guess.

In conclusion, laser scattering data on this experiment confirm previous interferometric density measurements as well as temperatures and densities computed in MHD simulations. The temperature is low as expected but high enough that the plasma pressure can be greater than the rf magnetic pressure. Through simulation we find that the extra particles known to exist at the end of the discharge enter the plasma during the application of the rotating magnetic field.

References

- BERNEY A., HEYM A., HOFMANN F. and JONES I.R. (1971)
Plasma Phys. 13, 611.
- HEYM A. (1968) Plasma Phys. 10, 1069.
- HOFMANN F. (1971a) Plasma Physics and Controlled Nuclear Fusion
Research, Vol I, p 267. International Atomic Energy Agency, Vienna.
- HOFMANN F. (1971b) LRP Report 46/71, this laboratory.
- IGNAT D.W., HEYM A., HOFMANN F. and LIETTI A. (1973)
Plasma Phys. 15,
- JONES I.R., LIETTI A. and PEIRY J.-M. (1968) Plasma Phys. 10, 213.
- KEGEL W.H. (1965) Report IPP 6/34, Institut für Plasmaphysik,
Garching bei München, West Germany.
- KUNZE H.J. (1968) "The Laser as a tool for plasma diagnostics", in
Plasma Diagnostics, ed. by W. LOCHTE-HOLTGREVEN, North-Holland
(Amsterdam). See page 588.
- TROYON F. (1971) Plasma Phys. 13, 715.
- WEIBEL E.S. (1960) Phys. Fluids 3, 946.

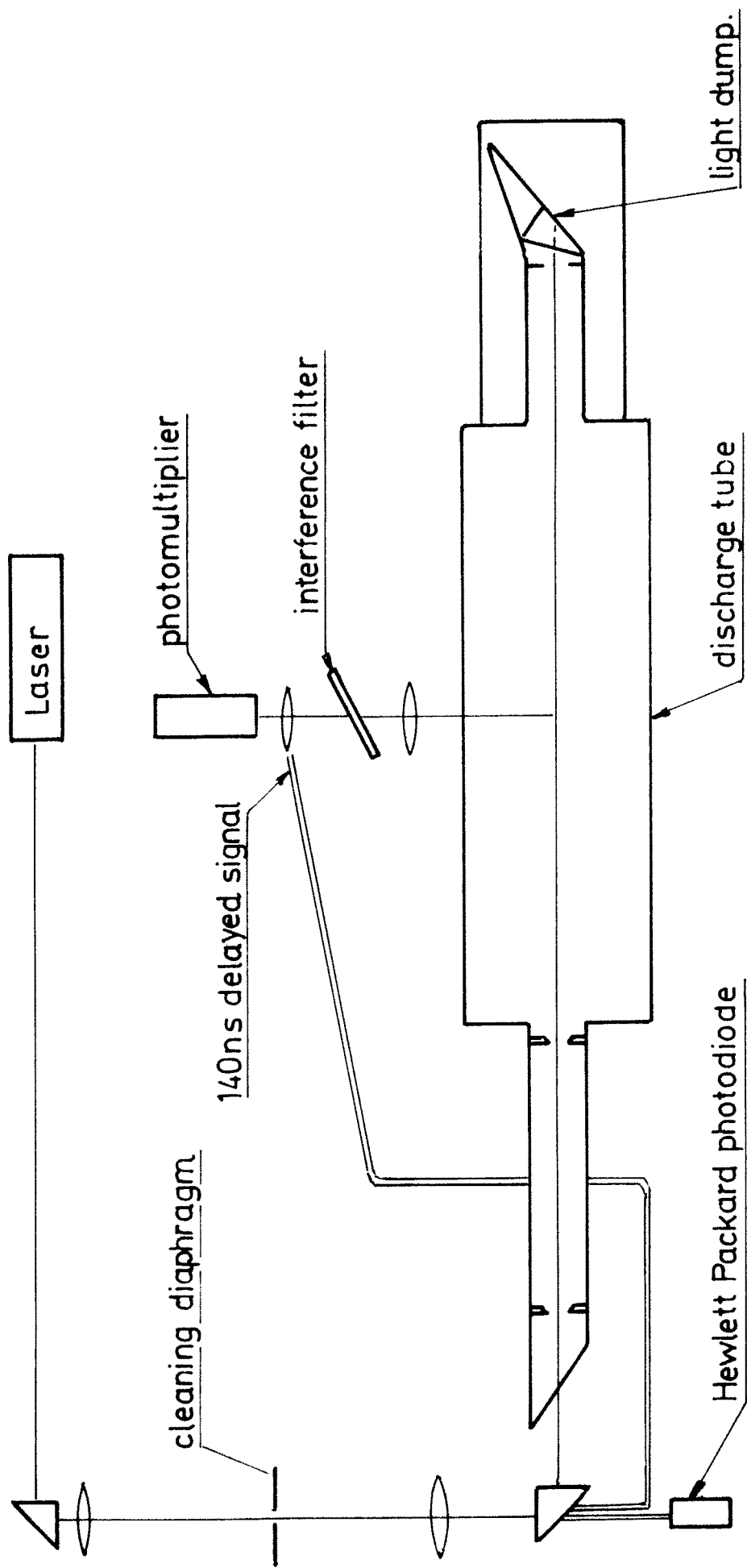
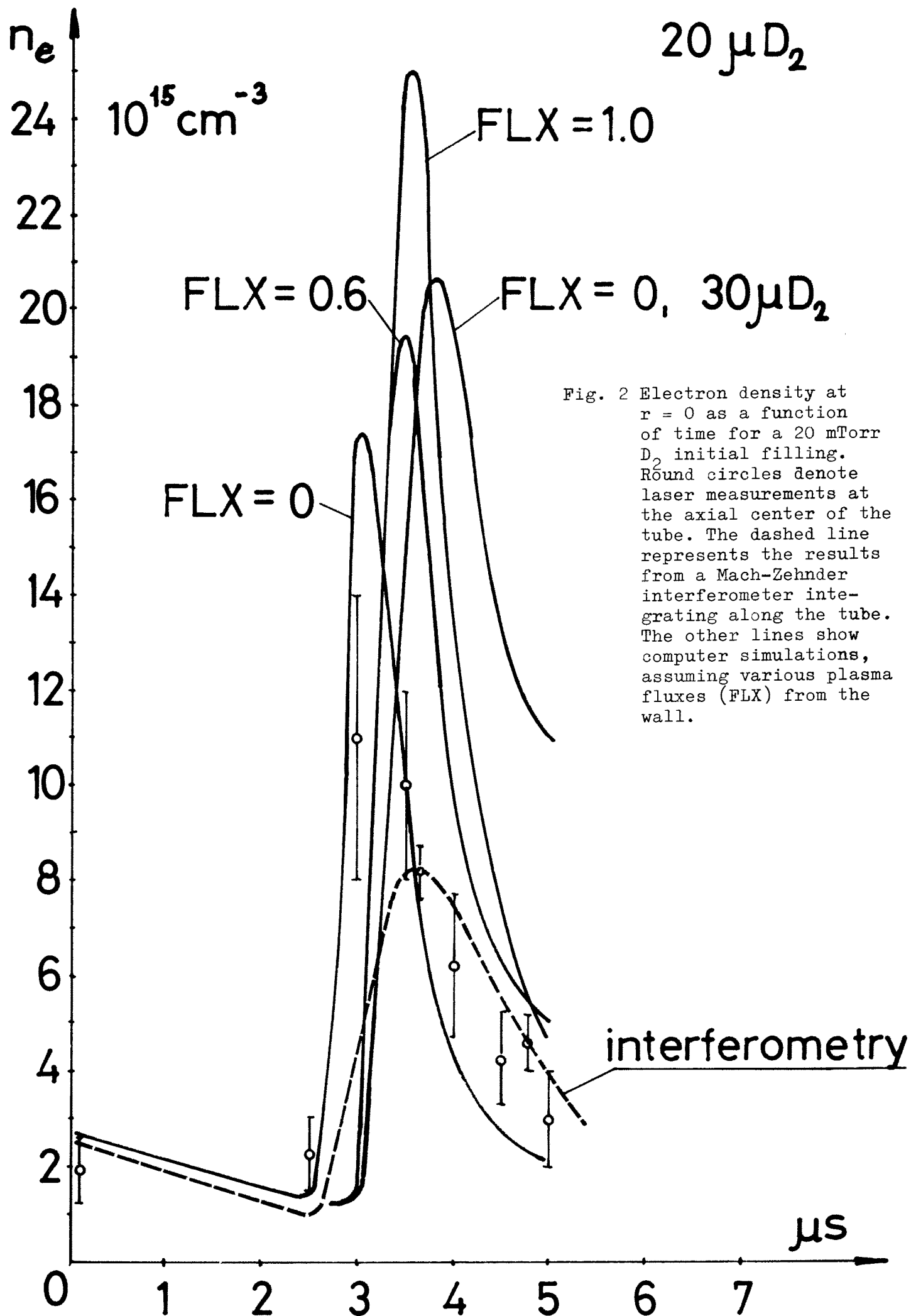


Fig. 1 Schematic diagram of the apparatus for the laser scattering measurement.



$20\mu\text{D}_2$

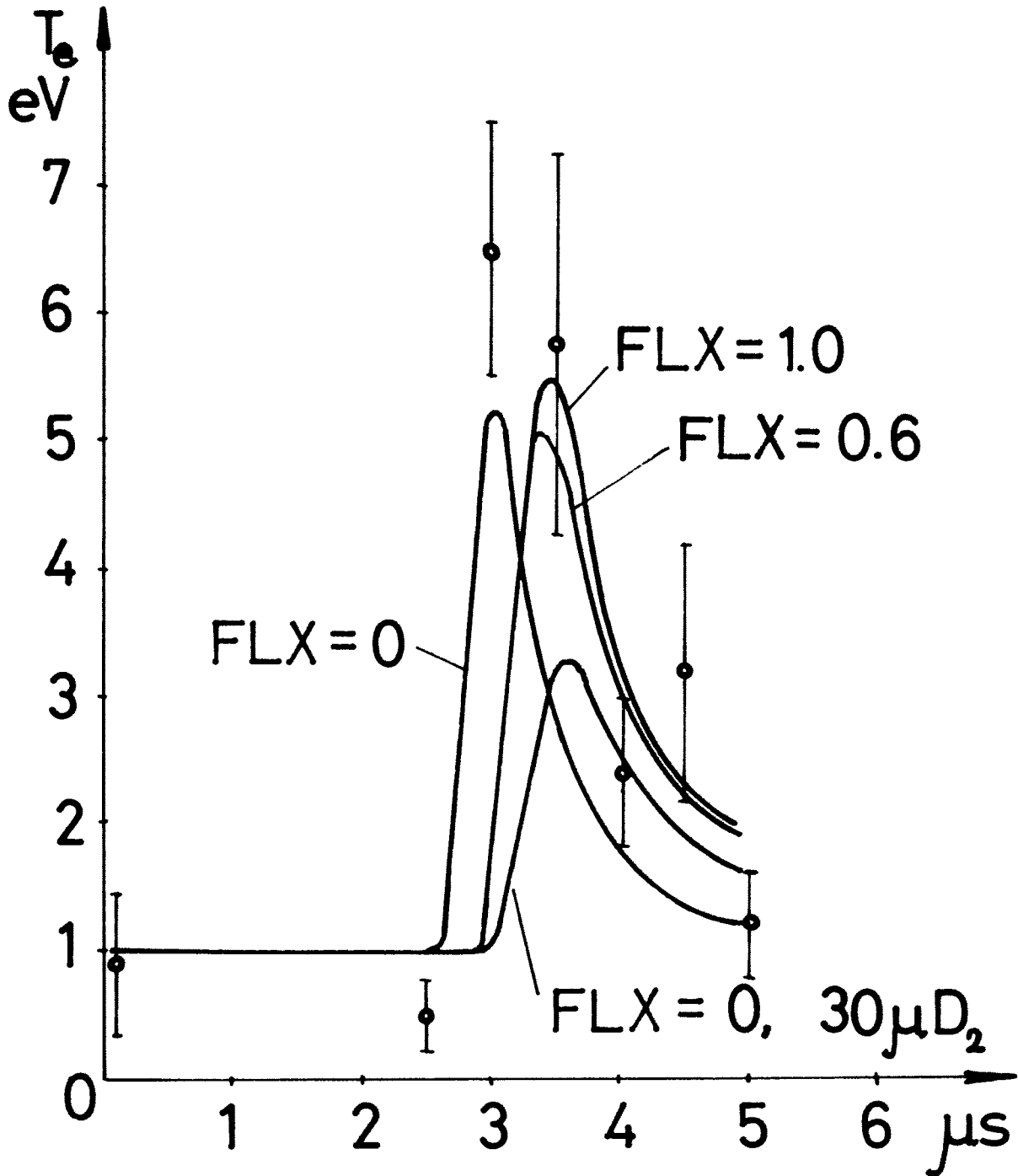


Fig. 3 Electron temperature at $r = 0$ as a function of time for a 20 mTorr D_2 initial filling. Round circles denote the scattering measurements at the axial center of the tube. The solid lines show computer simulations assuming various plasma fluxes (FLX) from the wall.

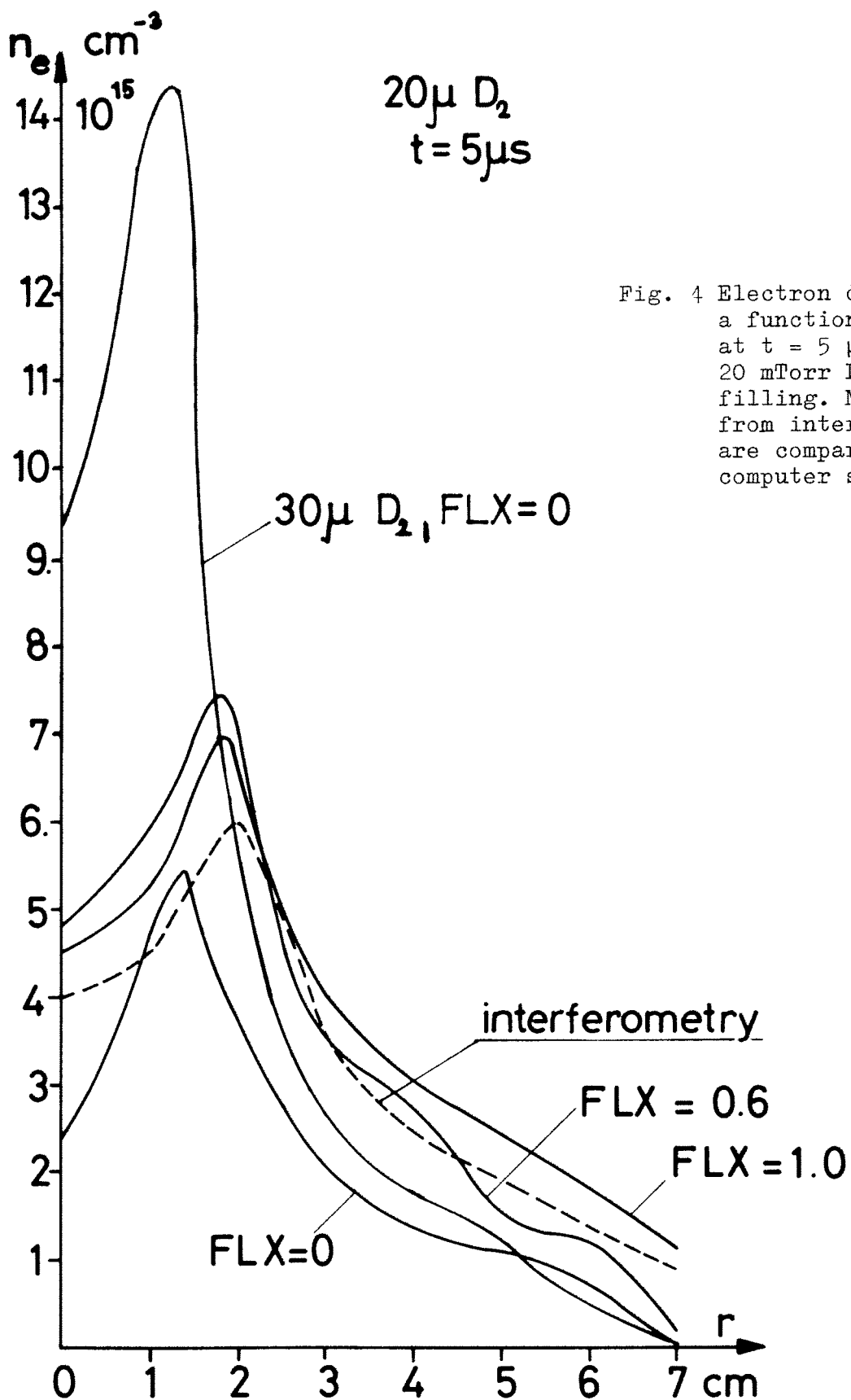


Fig. 4 Electron density as a function of radius at $t = 5 \mu\text{sec}$ for a 20 mTorr D_2 initial filling. Measurements from interferometry are compared with computer simulations.

